remote sensing

MDPI

Article

Recent Deceleration of the Ice Elevation Change of Ecology Glacier (King George Island, Antarctica)

Michał Pętlicki [1,2,*], Joanna Sziło [1], Shelley MacDonell [3], Sebastián Vivero [3,†] and Robert J. Bialik [1,4]

1 Institute of Geophysics, Polish Academy of Sciences, ul. Księcia Janusza 64, 01-452 Warsaw, Poland; jszilo@igf.edu.pl (J.S.); rbialik@ibb.waw.pl (R.J.B.)
2 Glaciology Laboratory, Centro de Estudios Cientificos (CECs), Av. Arturo Prat 514, 5110466 Valdivia, Chile
3 Centro de Estudios Avanzados en Zonas Aridas, Raul Bitran 1305, 1720010 La Serena, Chile; shelley.macdonell@ceaza.cl (S.M.); sebastian.viveroandrade@unil.ch (S.V.)
4 Institute of Biochemistry and Biophysics, Polish Academy of Sciences, ul. Pawińskiego 5a, 02-106 Warsaw, Poland
* Correspondence: petlicki@igf.edu.pl; Tel.: +48-22-691-58-94
† Current address: Institute of Earth Surface Dynamics (IDYST), University of Lausanne, Géopolis, Quartier Mouline, CH-1015 Lausanne, Switzerland.

Academic Editors: Frank Paul, Kate Briggs, Robert McNabb, Christopher Nuth, Jan Wuite and Prasad S. Thenkabai
Received: 2 March 2017; Accepted: 17 May 2017; Published: 24 May 2017

Abstract: Glacier change studies in the Antarctic Peninsula region, despite their importance for global sea level rise, are commonly restricted to the investigation of frontal position changes. Here we present a long term (37 years; 1979–2016) study of ice elevation changes of the Ecology Glacier, King George Island (62°11′S, 58°29′W). The glacier covers an area of 5.21 km^2 and is located close to the H. Arctowski Polish Antarctic Station, and therefore has been an object of various multidisciplinary studies with subject ranging from glaciology, meteorology to glacial microbiology. Hence, it is of great interest to assess its current state and put it in a broader context of recent glacial change. In order to achieve that goal, we conducted an analysis of archival cartographic material and combined it with field measurements of proglacial lagoon hydrography and state-of-art geodetic surveying of the glacier surface with terrestrial laser scanning and satellite imagery. Overall mass loss was largest in the beginning of 2000s, and the rate of elevation change substantially decreased between 2012–2016, with little ice front retreat and no significant surface lowering. Ice elevation change rate for the common ablation area over all analyzed periods (1979–2001–2012–2016) has decreased from -1.7 ± 0.4 m/year in 1979–2001 and -1.5 ± 0.5 m/year in 2001–2012 to -0.5 ± 0.6 m/year in 2012–2016. This reduction of ice mass loss is likely related to decreasing summer temperatures in this region of the Antarctic Peninsula.

Keywords: glaciology; ice elevation change; glacial retreat; DEM; Terrestrial Laser Scanning; Antarctica; South Shetland Islands

1. Introduction

Glacial retreat is a dynamic process largely influenced by the internal glacier dynamics [1,2], bedrock topography [3,4] and the response to climatic changes [5,6]. Even though the front position changes of fast flowing glaciers can be asynchronous to climatic forcing [3,7–9], over a long-term period, tidewater glacier termini retreat can be assumed to be an indicator of the atmospheric temperature rise [10,11]. Therefore, a globally observed retreat of glacial termini [12,13] is considered one of the most important indicators of climate change [14].

Since the 1950s, the Antarctic Peninsula region was subjected to an unprecedented air temperature rise of 0.03 °C/year [15]. This led to a large scale retreat of glacial fronts an rapid glacial change, including the disintegration of the Larsen A and B ice shelves [16,17]. However, it was shown by Turner et al. [18], Oliva et al. [19] that since 1999 a regional cooling has been observed, which has also influenced the behaviour of the cryosphere [19,20]. Air temperature records from the Bellingshausen Station (Figure 1; [21]) confirmed that for the 2012–2015 period a significant cooling was observed during summer months on the Fildes Peninsula, King George Island. Overall, the ice caps and glaciers of this region are one of the major sources of current sea level rise contributing 0.22 mm a^{-1} [22], compared to 0.47 ± 0.23 mm a^{-1} for the entire Greenland Ice Sheet between 1991–2015 [23]. Nonetheless, there is a large uncertainty concerning the volume change of glaciers in the Antarctic periphery, as the ground based measurements are relatively scarce [20,24].

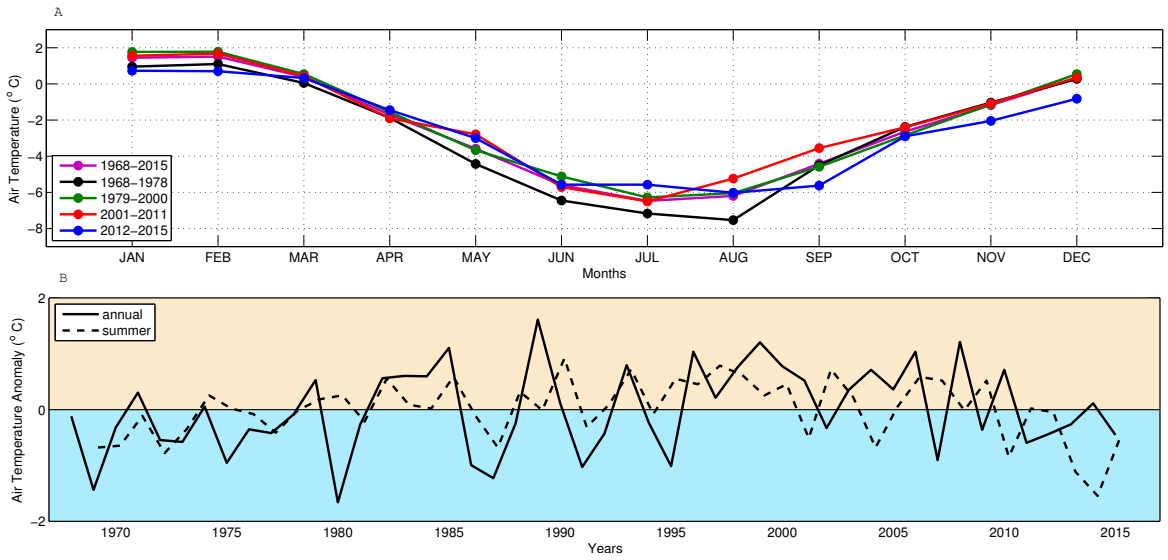

Figure 1. Air temperature at Bellingshausen Station (King George Island) during 1968-2015 period [21]. (**A**) Monthly means for time periods between acquisitions of DEMs of Ecology Glacier, (**B**) Annual and austral summer (Dec–Feb) air temperature means.

King George Island is the largest island in the South Shetland Islands archipelago (Figure 2a,b). A major part of the island is covered by an ice cap divided into five main ice basins: three connected domes along the main ridge (A-Bellingshausen, B-Arctowski and C-unnamed), and Kraków and Warszawa Icefields on the southern peninsulas [25]. Despite there being a number of published glacial extent change studies (e.g., [25–29]), only a few studies of glacier volume change in the South Shetland Islands area have been conducted (e.g., [20,26,30]). The majority of ice volume change studies covering this region are still based on volume-area scaling (e.g., [22,31]), with little in situ data that could provide robust validation. The study by [26] recorded surface lowering over the entire Bellingshausen Dome on King George Island, including at the summit, at 270 m a.s.l. However, given that the maximum elevation of the King George Island ice cap is much higher, approximately 700 m a.s.l. [25], there is a large uncertainty regarding overall volume change for the island, and mass balance modelling indicates that it is out of balance [32]. There have been several attempts to quantify the surface mass balance of King George Island glaciers (e.g., [28,32,33]) but little is known about their dynamic response and hence overall ice elevation change.

Located only 1 km south of the Arctowski Polish Antarctic Station, Ecology Glacier is the northernmost outlet glacier of Warszawa Icefield (Figure 2c), south of the ice-free area of Point Thomas Oasis. It calves into the Suszczewski Cove on the western coast of the Admiralty Bay. According to the Randolph Inventory, Ecology Glacier had an area of 5.21 km^2 and was 4.2 km long [34]. The bedrock topography of Ecology Glacier remains unknown, nonetheless it can be assumed that subglacial

relief is highly complicated with multiple subglacial landforms, as has been observed beneath the neighbouring Bellingshausen and Arctowski Icefields [35,36]. This assumption can be supported by the presence of significant undulations of the ice surface of the glacier. The glacier has been a subject of interdisciplinary research for almost 40 years, including studies of glacier mass balance [28,33], glacio-meteorology [37] and glacial microbiology [38,39]. Although the mass balance [28,33] and ice extent change over several periods has been reported elsewhere [26,28,40–42], a detailed assessment of ice elevation change is still lacking.

The main goals of this paper are to quantify ice elevation change of Ecology Glacier, an outlet glacier of King George Island ice cap between 1979 and 2016, and to partition ice elevation changes related to frontal retreat and surface lowering.

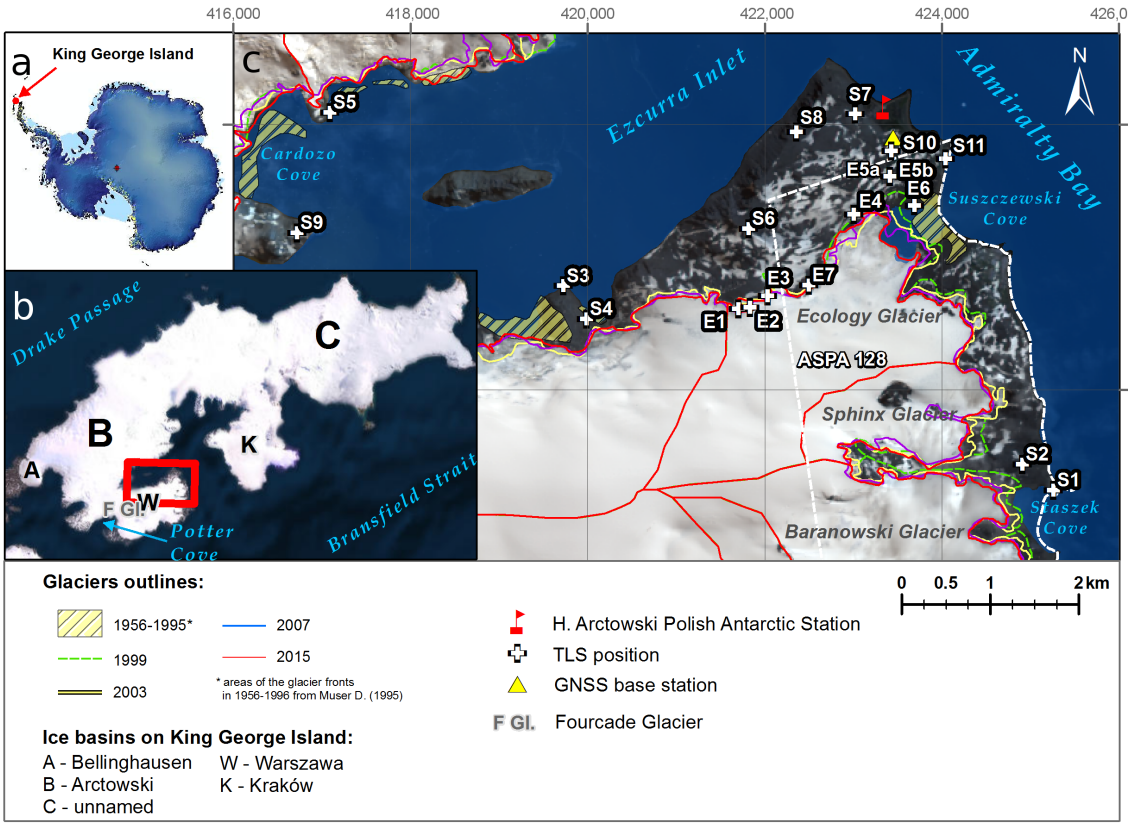

Figure 2. Map of the study site: (**a**) Location of King George Island; (**b**) location of Ecology Glacier; (**c**) Ecology Glacier and surroundings (indicated by red box). Basemap is a Landsat image acquired on 18 January 2014. Reference system: WGS 1984, UTM zone 21S, geoid EGM96.

2. Materials and Methods

This study computes ice elevation changes by differentiating Digital Elevation Models (DEMs) constructed using archival maps, aerial panchromatic images, high-resolution satellite imagery, terrestrial laser scanning and bathymetric data.

2.1. 1979 DEM—Aerial Photographs

During the austral summer of 1978/1979, a series of airborne imagery was taken to map the Admiralty Bay area [43]. These images were subsequently used by Pudełko [44] to create an orthophotomap of Antarctic Specially Protected Area (ASPA) 128. 1:3600 scale images were taken with a spy camera AFA-21 mounted on a Mi-2 helicopter. The original images were scanned by Pudełko [45] and stored in digital format. Agisoft Photoscan was used to orthorectify

14 photographs and to create a 3D model of the terminal section of Ecology Glacier and the ice-free area north of it using the Structure-from-Motion method [46,47]. Twenty two ground GCPs located on bed outcrops and Arctowski Station buildings were used for georeferencing, their positions were measured on the 2016 DEM and yielded a mean elevation error of 2.43 $\pm$ 7.24 m.

2.2. 2001 DEM and Archival Maps

Three maps were used as the basis for this study: (1) 1:50,000 scale topographical map of the Admiralty Bay [43] that was further improved with topographic works conducted in 1988/89 [48]; (2) 1:12,500 scale topographical map of SSSI-8, now called ASPA 128 [45]; and (3) 1:10,000 scale orthophoto map of Western Shore of Admiralty Bay, King George Island, South Shetland Islands [44]. For construction of the DEMs based on maps [44,45], the original isolines were provided and used, while isolines on the 1990 map were digitized manually in ArcGIS. The DEM for 2001 was computed in ArcGIS software by the TopoToRaster interpolation of contours taken from a 1:12,500 topographical map [45], based on data collected during the XXV Antarctic Expedition (2000/2001) with use of two double frequency GPS receivers Ashtech Z-12. According to [45], the precision of surveyed points was better than 100 mm. However, in some cases obtaining the points was impossible because of the loss of communication with satellites or due to difficult terrain. In these situations, gaps were interpolated based on aerial photos from 1979 and theodolite measurements (for more details see [45]).

Maps [43,48] have large distortions and could not be used for the purpose of this study. For further analysis only the maps of [44,45] were used, for which the interpolation error was calculated as the elevation difference with 2016 DEM over unglaciated areas of Point Thomas Oasis north of Ecology Glacier, yielding mean elevation error of 1.26 $\pm$ 6.61 m. However, it cannot be excluded that the error over ice-covered areas might be higher.

2.3. 2012 Pléiades DEM

The DEM for the lower Ecology Glacier, and surroundings, derived for 2012 was based on an along-track, tri-stereo set of Pléiades 1A panchromatic images collected on 25 December 2012 (Centre National d'Etudes Spatiales, Paris, France) and a set of six ground control points (GCPs). The tri-stereo set was selected because it presented the lowest percentage of cloud cover for available images during the 2012/13 summer, and it only contains a small seasonal snow coverage which facilitates the delineation of the glacier. For DEM construction, the original 12 bit encoding of the panchromatic band was used instead of the optional 8 bit encoding, as the former provided improved image contrast over flat and featureless areas of the glacier [49,50].

The GCPs used to refine the DEM from relative to absolute elevations were collected in December 2015 utilizing a Trimble Zephyr antenna and Pathfinder ProXRT receiver differential GPS (dGPS) system (Trimble Inc., Sunnyvale, CA, USA). The mean horizontal and vertical precision of the GCPs were 0.19 m and 0.21 m, respectively, which were largely influenced by poor satellite configuration due to the latitude, even though occupation times were relatively long (10–20 min).

A bundle-adjustment was undertaken using Imagine Photogrammetry 2014 software (Hexagon Geosystems, Heerbrugg, Switzerland), which incorporated the panchromatic images, the six GCPs, forty tie points and the initial orientation data of each image from the original Rational Polynomial Coefficients (RPCs). The overall accuracy of the tri-stereo bundle-adjustment was a root mean squared error (RMSE) of 0.45 pixels ($\sim$0.25 m). An automatic DEM extraction procedure was employed with all geometric parameters associated with the three overlapping images, by matching conjugated points from image overlaps and retrieving their 3D coordinates. It is important to note that by using triplet matching, redundancy is introduced into the derivation of elevation which improves the accuracy of the final DEM product [50]. Finally, the irregularly distributed 3D points were interpolated to a raster grid DEM using a non-linear interpolator with a sampling resolution of 0.5 m.

2.4. 2016 Terrestrial Laser Scanning DEM

In the austral summer 2015/2016, a detailed survey of the main trunk of Ecology Glacier and its surroundings was made with a Riegl VZ-6000 long-range terrestrial laser scanner (RIEGL Laser Measurement Systems GmbH, Horn, Austria). The measurement principle of this instrument is time-of-flight with online waveform processing. This instrument is characterized by a very long effective range over the ice and snow surfaces due to the used wavelength of the laser beam (1065 nm) and has been used in various glaciological applications (e.g., [51,52]). The glacier surface was surveyed from seven positions (Figure 2, Table A1): three near the front (Ecology E, N and S), one near the equilibrium line (Wróbel Hill) and three overlooking the accumulation zone (Dutkiewicz Cliff E, N and S) on three separate dates: 27 January, 17 and 21 March, 2016. The position of the Terrestrial Laser Scanner (TLS) was measured with a differential GNSS (GPS+GLONASS) receiver Leica GS14. The base station (Leica GS10 receiver) was located at Jasnorzewski reference point in the vicinity of Arctowski Polish Antarctic Station (Figure 2, Table A1). Measurements were made in static mode and post-processed with Leica Geo Office software, yielding mm-scale 3D accuracies. As the glacier surface could only be surveyed from the northern side of the glacier, a series of additional TLS surveys of the surrounding terrain was conducted in order to increase the accuracy of georeferencing (Figure 2). This provided a larger baseline (4269 m in N-S and 8546 m in E-W direction) for the survey, decreasing the georeferencing error.

TLS data was processed with RIEGL RiSCAN PRO, a proprietary software provided by the manufacturer of the scanner. First, point clouds were processed with the Multiple-Time-Around (MTA) package to account for long-range multiple echoes enhancing the effective range of the measurements to 6000 m. Next, artifacts due to reflection from the presence of falling snow during the data acquisition, reflection from sea surface and sea ice present in Suszczewski Cove were removed. Snow and ice surfaces were eliminated manually from point clouds. Subsequently, all point clouds were aligned into a common global coordinate system using the Multi-Station Adjustment (MSA) plugin. The overall georeferencing error as reported by the MSA plugin was 85 mm. Finally, point clouds were merged into one polyobject, exported to the LAS data format (American Society for Photogrammetry and Remote Sensing LASer file format), and interpolated to a 1×1 m rectangular grid with CloudCompare software, resulting in a DEM of Ecology Glacier and its surroundings.

2.5. Proglacial Lagoon Echosounding and Sediment Sampling

Lagoon bathymetry data were collected during March 2016 using a float-mounted acoustic Doppler current profiler (ADCP, RiverSurveyor S5, manufactured by SonTek, San Diego, CA, USA). This device was equipped with a vertical single-beam echo sounder (working at a frequency of 1 MHz and accuracy 1% of measuring values), and four-beams (working at a frequency of 3 MHz, with 25° slant angle and accuracy 0.25% of measuring values), enable the 3D visualization of "surface" water velocity. The dGPS provides the ADCP horizontal position with an accuracy of 0.5 m.

Measurements were made along the survey lines on 2, 17, 21 and 29 March 2016 with a total surveyed length of approximately 20 km (see Figure 3). It should be noted, however, that the Admiralty Bay experiences significant tides with maximum amplitudes of 1.81 m. Therefore, it was important to take account the short-term tidal level changes during the day of measurement. Table 1 shows the water level during the start and the end of the field work, which were obtained from the numerical data available at www.tide-forecast.com. Due to the small differences of up to 0.2 m, we assumed linear model changes, and the obtained values were treated as an amendment to the measured values of bathymetry. They were all related to a depth of 0.7 m as a reference point.

The measured depths refer to the present geometry of the lagoon (2016), but it could have been deeper in the past if the marine or glacial sedimentation has decreased its depth over time. While glacial sedimentation rates in this area are relatively well constrained (e.g., [53]), the marine sedimentation rate is unknown and can provide additional source of uncertainty in long-term lagoon bathymetry estimation. Therefore, in order to determine the presence and origin of sediments in the lagoon,

sediment samples were collected from three locations: (1) close to the front of the glacier; (2) in the central part which is close to the islands; and (3) finally in the small bay (Figure 3). For each of these cases, the samples were taken with use of Ekman bottom grab and at least 1 kg of bed material was collected for further analysis and determination of granulometric distribution curves.

Table 1. Main characteristic of the Ecology Glacier lagoon echosounding.

Date	Track Length (m)	Number of Samples	Sea Level		Sea Surface Temperature (°C)
			Start (cm)	End (cm)	
2 Mar 2016	5928	5046	114	110	4.41
17 Mar 2016	2293	2080	120	116	1.05
21 Mar 2016	4011	3938	116	136	0.58
29 Mar 2016	7593	4774	131	112	1.16

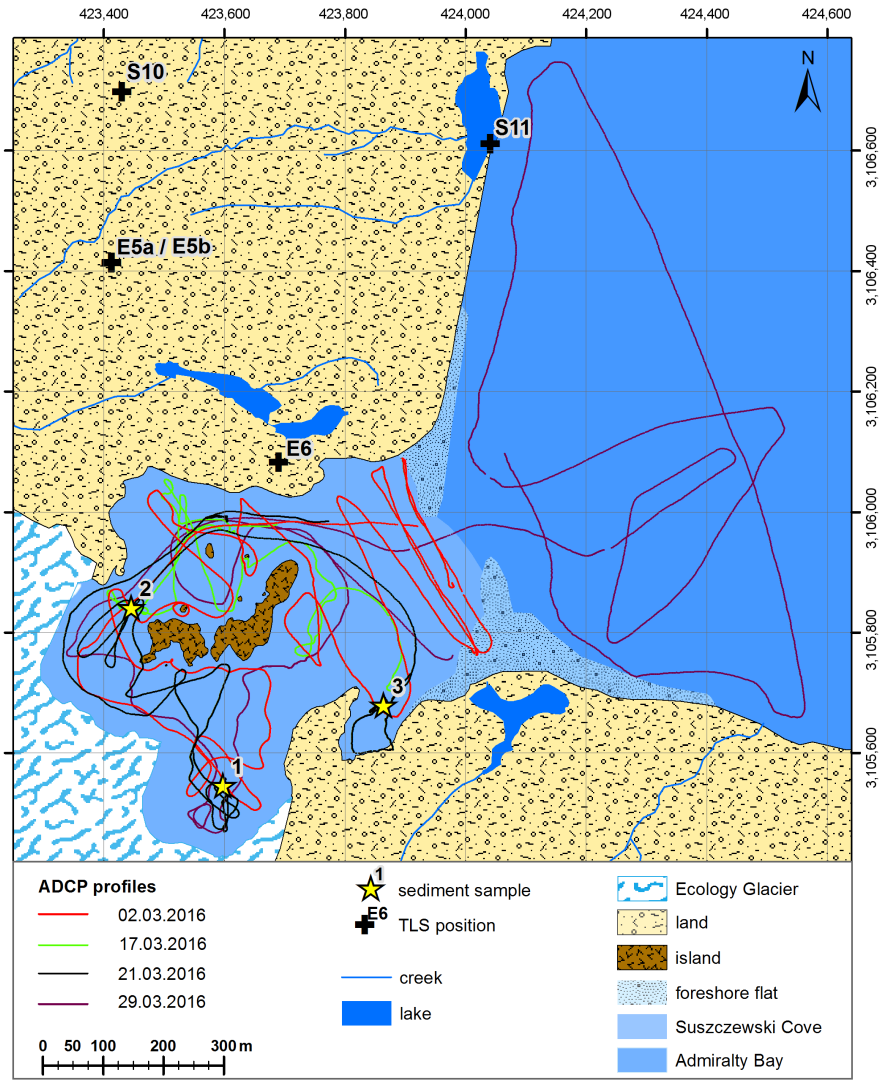

Figure 3. Profiles of ADCP measurements in Suszczewski Cove in March 2016. Reference system: WGS 1984, UTM zone 21S, geoid EGM96.

2.6. DEM Differencing and Ice Elevation Changes

Ice elevation changes were computed by differencing subsequent DEMs for each time interval (e.g., [54–56]). Each DEM was interpolated into a common reference system and grid, co-registered

with use of several GCPs derived from the 2016 TLS DEM. Then, ice elevation change was computed as the difference in height over the glaciated area. Given that the lagoon bathymetry was only known for 2016, it was assumed that it reflects the same level as the glacial bed when it was still covered by ice. Such assumption is supported by relatively low (6.6 mm a^{-1}) sediment accumulation rates reported for another outlet glacier of the Warszawa Icefield, the Fourcade Glacier [53].

3. Results

3.1. Digital Elevation Models

Only the terminal section of the Ecology Glacier is covered by the 1979 DEM due to relatively small overlaps between the aerial images and their oversaturation on snow surfaces resulting in few identifiable features that could serve for image pair matching. As presented in Figure 4, frontal position in 1979 was close to the border of Admiralty Bay, with an ice cliff height of approx. 45 m. The glacier surface was quite smooth and the glacier covered almost the entire area of present proglacial lagoon. In 2001, the front had retreated to the rocky outcrops in the middle of Suszczewski Cove, and the surveyed ice surface was 290 m a.s.l. in the region between Zamek and Dutkiewicz Cliff. Between 2001 and 2012 significant terminus retreat was again observed, forming almost half of the present proglacial lagoon in Suszczewski Cove. This subset covers the entire Ecology Glacier, up to the ice divide on the Warszawa Icefield. The 2016 glacier DEM is restricted to the main trunk of Ecology Glacier and partly reaches the ice dome of Warszawa Icefield.

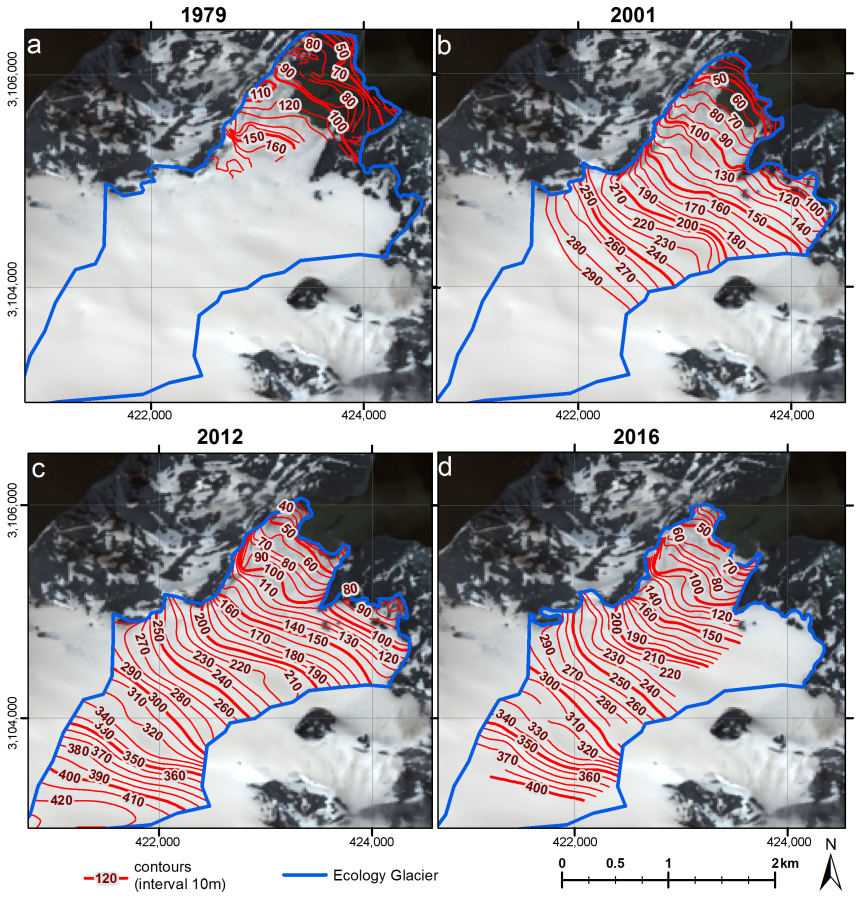

Figure 4. The surface elevation of Ecology Glacier: (**a**) 1979, (**b**) 2001, (**c**) 2012 and (**d**) 2016. Basemap is a Landsat image acquired on 18 Jan 2014. Reference system: WGS 1984, UTM zone 21S, geoid EGM96.

The quality of the produced DEMs was analyzed by computing elevation differences over non-glaciated areas of Point Thomas Formation, north of the terminal part of Ecology Glacier (Table 2). As the TLS was the most precise method of DEM creation used in this study, the 2016 DEM was used as a reference for DEM comparison (see Figure 5). The 1979 DEM has largest standard deviation of elevation difference of 9.70 m, while the maximum elevation difference was almost 60 m over steep areas of rock cliffs surrounding Ecology Glacier. The 2001 DEM showed a smaller standard deviation of elevation difference (6.61 m), however maximum differences remain very high (over 50 m). Again, this can be explained by rough topography and low spatial resolution of the original cartographic material [45]. As the Ecology Glacier surface generally have gentle slopes, such high values of maximum errors should not influence the quality of glacial DEMs and, thus, the calculated ice elevation changes. The 2012 Pléiades DEM have much smaller standard deviation of the elevation difference than other datasets used (1.27 m), and the mean difference is positive at 0.5 m. This can be explained by the significant presence of snow cover in Point Thomas Oasis in the austral summer 2012/2013 when Pléiades imagery was acquired.

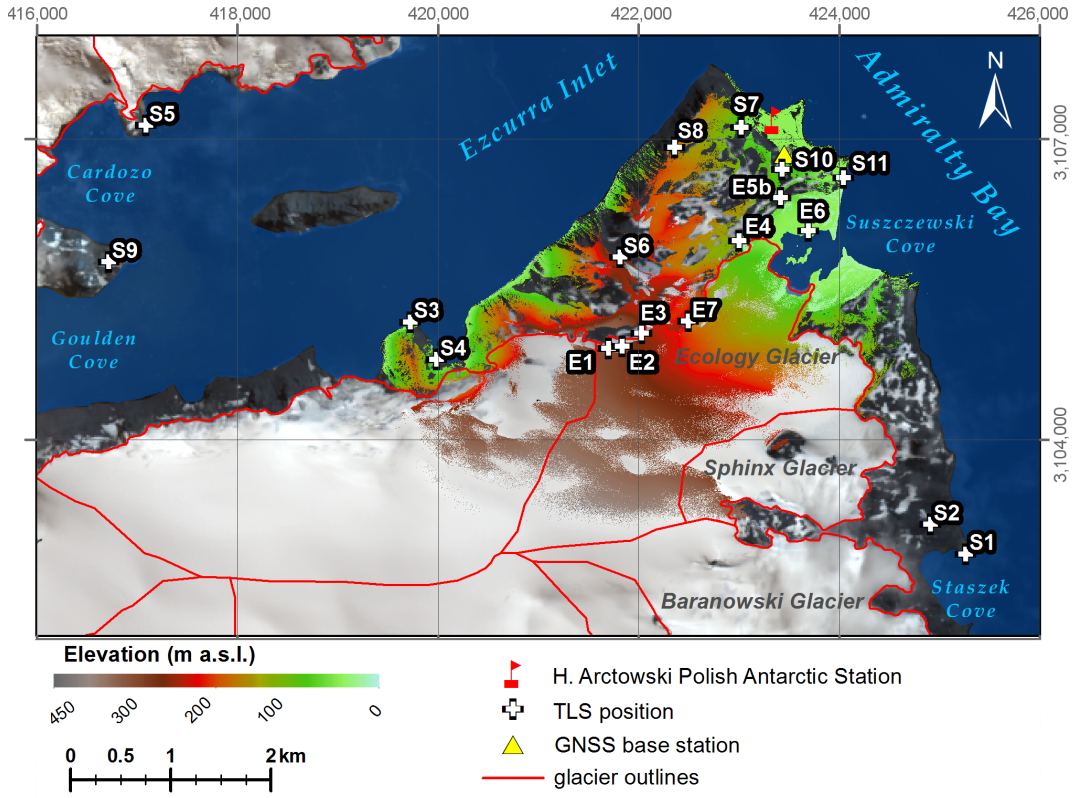

Figure 5. The surface elevation of Ecology Glacier and Point Thomas Oasis surveyed with TLS in March 2016. Reference system: WGS 1984, UTM zone 21S, geoid EGM96.

Table 2. DEM errors relative to 2016 TLS DEM, estimated as elevation difference over non-glaciated area of Point Thomas Oasis.

DEM	Mean Difference (m)	Standard Deviation (m)	Max Difference (m)	Min Difference (m)
2012	+0.48	1.27	+24.42	−15.96
2001	+1.26	6.61	+27.12	−53.32
1979	+2.87	9.70	+58.85	−40.71

3.2. Pro-Glacial Lagoon Echosounding

The entire area of the proglacial lagoon of Ecology Glacier was equal to 0.296 km^2 in 2016. Its mean depth was 3.6 ± 1.9 m and the maximum depth of 11.83 m was measured in the southern part near the front of the glacier (Figure 6). The lagoon is separated into two parts by a relatively shallow area which contains several small islands (rock outcrops). We speculate that the maximum depth is connected with subglacial outflows of fresh water which were observed during the field campaigns and can be identified as sources of cold water in the surface temperature maps (Figure 7).

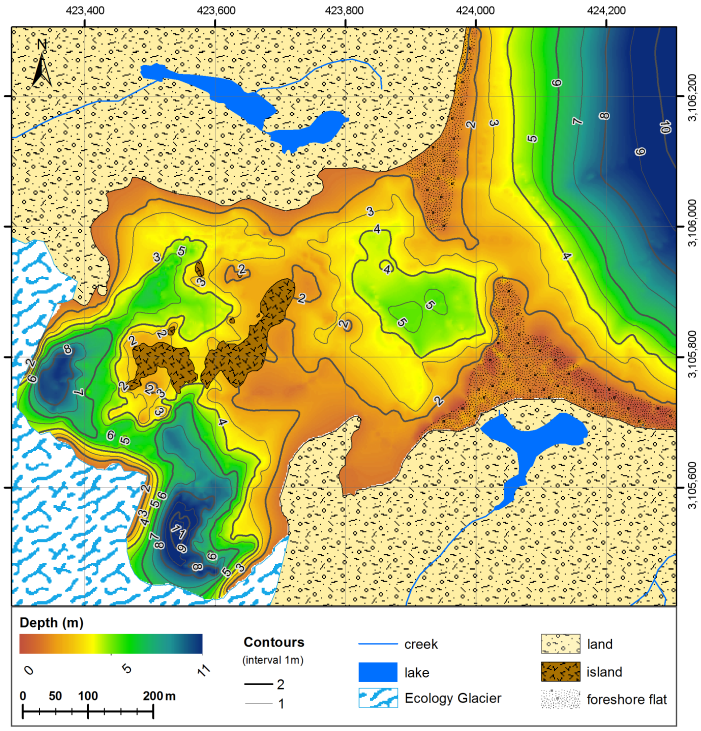

Figure 6. Bathymetry of Suszczewski Cove in March 2016.

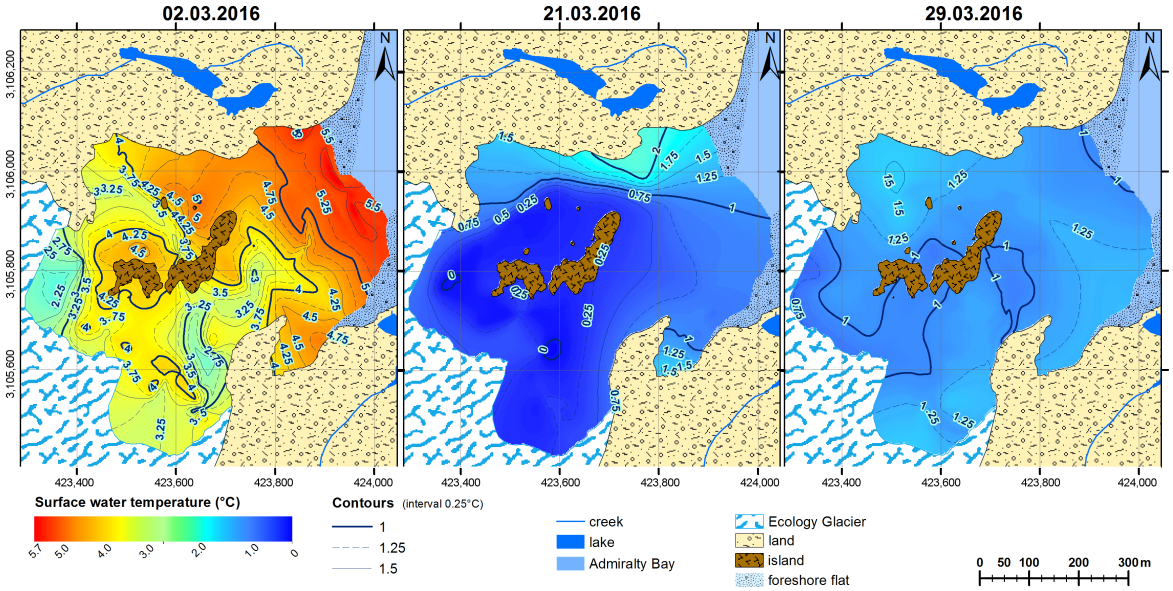

Figure 7. Temperature of proglacial lagoon in March 2016.

Figure 8 shows granulometric distribution curves of the bed sediment displaying all considered cases. Close to the front of the glacier the bed material consists mostly of silt (from very fine to coarse) with D16 = 0.0007 mm, D50 = 0.0205 mm, and D84 = 0.2760 mm whereas within the small bay (see Figure 3) it consisted of sand (from medium to coarse) and fine gravel with D16 = 0.0024 mm, D50 = 0.2160 mm, and D84 = 5.9600 mm. In contrast, the bed material close to the islands located in the central part of the Suszczewski Cove consisted mostly of very fine, fine and medium sand with D16 = 0.0011 mm, D50 = 0.2705 mm, and D84 = 2.5200 mm. These values imply that the sediment in the inner part of the proglacial lagoon can be associated with subglacial outflow deposits, while the sediment collected in the outer part has marine origin.

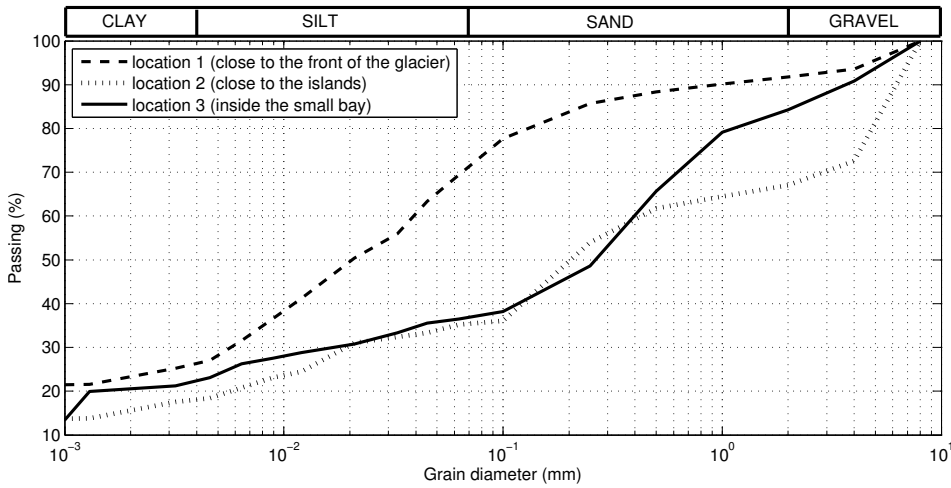

Figure 8. Granulometric distribution curves of bed sediment in proglacial lagoon of Ecology Glacier.

3.3. Ice Elevation Changes

Ice elevation change, calculated by differencing respective co-registered DEMs, shows large spatial and temporal variability (Figure 9, see also Figure A1). The largest elevation changes were observed in the areas where the ice front retreated due to calving, whereas changes caused by surface lowering due to melt were much smaller. There is a sharp increase in ice elevation change at the calving front position. The surface of the upper part of the glacier remains relatively stable, especially for the 2012–2016 period, when almost no surface lowering was observed not only above the equilibrium line of 150 m a.s.l. reported by Sobota et al. [28], but also higher than the speculated ELA of 230 m a.s.l on the Fourcade glacier [57] located in the Potter Cove (Figure 2). Over the entire 1979–2016 period, the Ecology Glacier lost more than 100 m of ice thickness in its terminal part affected by the front retreat. Adjacent area that is still covered by ice lost ∼60 m, which implies that remaining 40 m (approximately 40%) must have been caused by the calving front retreat (Table 3).

Table 3. Ice elevation changes of Ecology Glacier for the common area over all analyzed periods (1979–2001–2012–2016).

Period	Mean Ice Elevation Change (m)	Mean Ice Elevation Change Rate (m/Year)
2012–2016	-1.6 ± 1.9	-0.5 ± 0.6
2001–2012	-18.0 ± 5.8	-1.5 ± 0.5
1979–2001	-38.4 ± 9.1	-1.7 ± 0.4
1979–2016	-57.9 ± 10.1	-1.6 ± 0.3

The largest rate of elevation change is associated with regions of frontal retreat where the entire ice thickness is removed over a relatively short period of time due to calving (Figure 9). Comparison of ice elevation change for a common area over all analyzed periods shows that the ice surface elevation rate has been relatively stable around -1.6 m/year between 1979 and 2012 (Table 3).

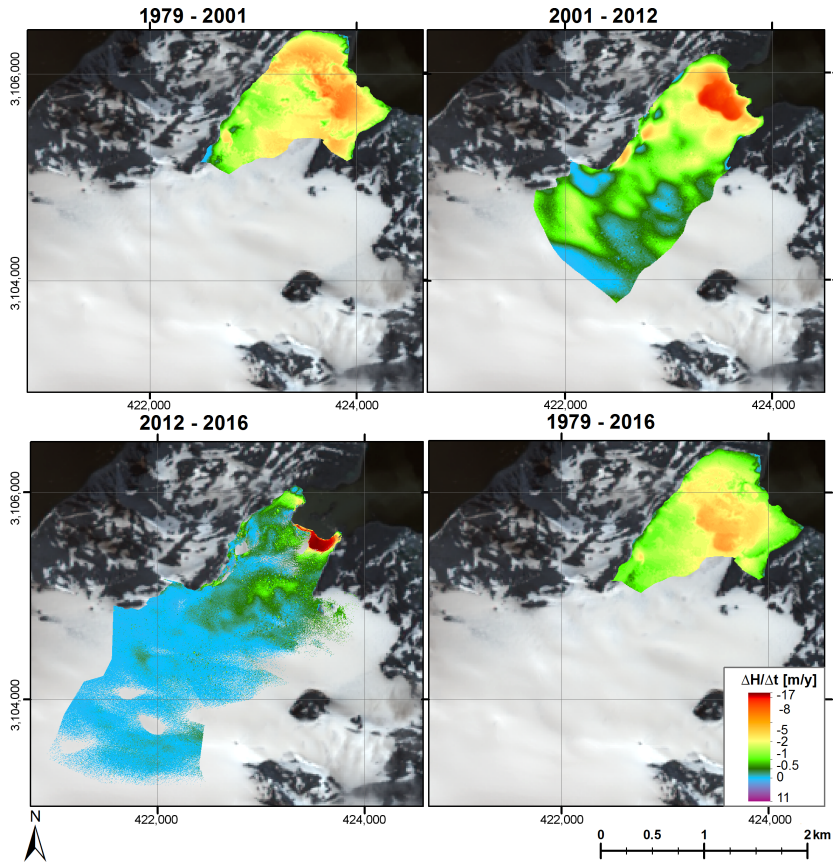

Figure 9. Rate of surface elevation change of Ecology Glacier 1979–2001–2012–2016. Reference system: WGS 1984, UTM zone 21S, geoid EGM96.

The ice front position was relatively stable and the retreat rate was low in the years 1956–1979, 1999–2003 and 2012–2016, when the front terminated near bedrock outcrops (Figures 10 and 11). The highest rate of frontal retreat was observed in years 1979–1988 and 2007–2012, when the ice cliff was standing in relatively deep water. Over the period 2001–2016, the ice elevation change was very low along the central line of Ecology Glacier above 250 m a.s.l. (Figure 10).

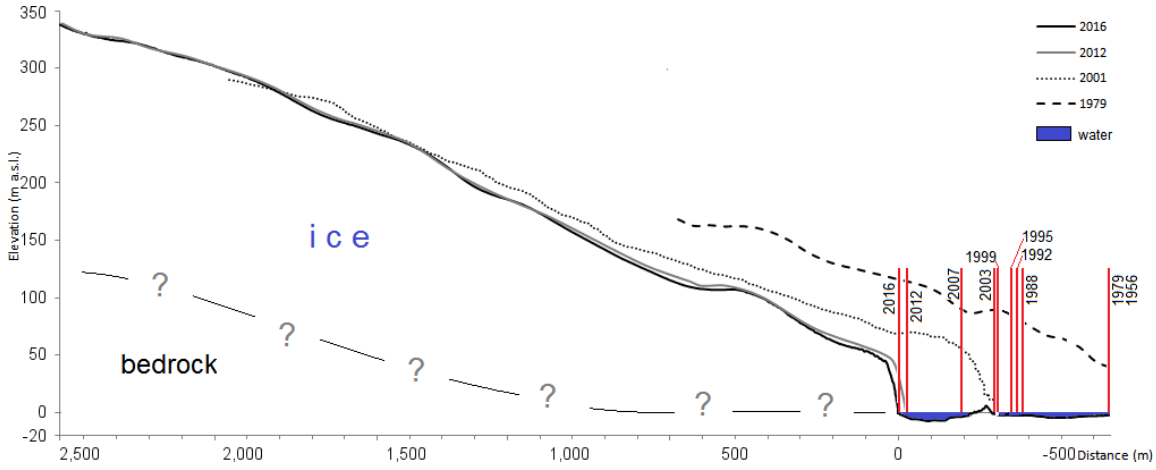

Figure 10. Bedrock elevation along a center line cross section of the Ecology Glacier with marked front position in 1979–2001–2012–2016.

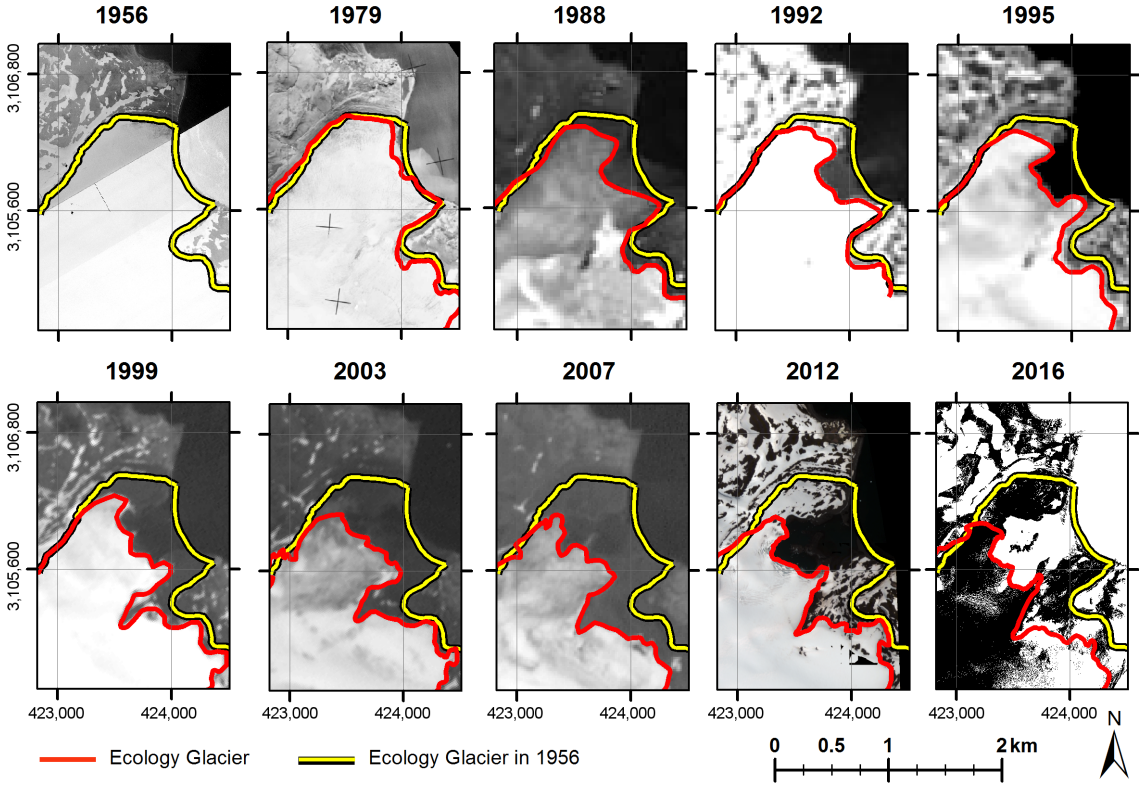

Figure 11. Ecology Glacier front positions in 1956–2016 period derived from aerial (1956–1979) and satellite imagery (1988–2012) and TLS (2016). Reference system: WGS 1984, UTM zone 21S, geoid EGM96.

4. Discussion

An important shift in the ice elevation change of Ecology Glacier was detected in years 2012–2016, when both frontal retreat and surface lowering due to ablation have decreased. This can be partially explained by observed positive surface mass balance, at least over the season 2012/2013 [28]. Whereas the surface elevation change is close to zero, the ice front retreat reported by [26] is still ongoing, although it has decelerated. The boundary between ice elevation loss and gain over the years 2012–2016 is located at the elevation of 200 $\pm$ 25 m a.s.l., slightly above the recent ELA of 150 m a.s.l. reported by Sobota et al. [28]. While these two values cannot be directly compared, as the former includes the ice dynamics component (emergence/subsidence flux) and the latter does not, this indicates that the glacier is currently out of balance in its ablation zone.

On neighbouring Livingston Island ice cap, a significant deceleration of the mass loss caused by positive surface mass balance, has also been reported and associated with air temperature change [20]. Comparatively, in the case of the Antarctic Peninsula outlet glaciers, the major fraction of ice elevation changes have been attributed to frontal retreat, with little contribution of ice surface lowering [12]. On the contrary, only ~40% of the ice elevation loss in the terminal part of Ecology Glacier can be attributed to the long-term frontal retreat (Table 3). This can be explained by the shallow depths of the proglacial lagoon that do not contribute significantly to the overall ice cliff height. On long term, this limits the contribution of frontal retreat to ice elevation change to approximately 40 m. Hence, long-term ice elevation change has to be driven mainly by surface melt and ice dynamics. Surface melt is directly dependent on climate and should decrease with recently observed cooling (Figure 1, while ice dynamics should indirectly respond to decreasing ice thickness, increased slope and change in sliding speeds caused by varying supply of meltwater to the glacier base.

Locations where the Ecology Glacier ice front position was relatively stable and the retreat rate was low coincide with a presence of the bedrock outcrops (Figure 10), indicating that the glacier retreat may be governed by the presence of pinning points [58]. Despite shallow depths of the proglacial lagoon, it seems that the water depth controls termini retreat rate through enhanced calving. This may be caused by undercutting of the ice cliff [59–61] by relatively warm water, reaching 4 °C (Figure 7). However, given that the elevation change caused by front retreat is limited by low ice cliff height due to small water depths, this should not affect the interpretation of long-term climate effects.

Proglacial lagoon bed sediment granulometry (Figure 8) suggests that the bottom sediment in the outer part of proglacial lagoon is maritime whereas the one located near the glacier front is a product of local glacial sedimentation. This may be the result of backfill of the Suszczewski Cove and higher influence of the marine processes on the outer part of the proglacial lagoon, principally the Bransfield Strait swell entering the lagoon and depositing coarse sediment. Consequently, this can lead to an erroneous estimation of the bedrock depth when the lagoon was still covered by ice and thus constitute a possible source of underestimation of the calculated ice elevation change in this area.

Although the 1979 DEM reconstruction from aerial photos and the 2001 map [45] have relatively large errors (Table 2), the observed glacier elevation changes are typically an order of magnitude higher (Figure A1, Table 3). Thus, as recently shown by [47], performing Structure-from-Motion analysis of archival aerial imagery can be a valuable source of information concerning long-term glacial change.

The Warszawa Icefield shows generally low dynamics comparing to other parts of the King George Island and is not contributing significantly to the overall mass balance of the entire ice cap of King George Island [27]. Therefore it is more sensitive to the surface mass balance changes than to ice flow variations, showing a more direct response to climate signals than the more dynamic neighbouring icefields. Our data shows slight thickening in the accumulation area in recent years (2012–2016). Unfortunately, it was not possible to determine previous elevation change in the upper reaches of Ecology Glacier due to an insufficient spatial coverage of produced DEMs.

It must be stressed that the mass balance of glaciers on King George Island is highly dependent on the large-scale circulation, mainly by advection of warm, humid air from the north [62]. Therefore, it is important to consider long term changes that are independent of the short-term fluctuations. Whereas recent years showed significant air temperature cooling and thus positive net surface mass balance, future changes of climate in the region are not clear given its high natural variability [18].

5. Conclusions

Ecology Glacier experienced highly negative mass balance over 1979–2016 driven both by high surface melt and frontal retreat. The ice elevation change rate for the common ablation area over all analyzed periods (1979–2001–2012–2016) has changed from -1.7 ± 0.4 m/year in 1979–2001 and -1.5 ± 0.5 m/year in 2001–2012 to -0.5 ± 0.6 m/year in 2012–2016.

Ice surface lowering of Ecology Glacier has significantly decelerated in the beginning of the 21st century, especially in 2012-2016 when the glacier was close to equilibrium. Ice flow velocities of the terminal part of Ecology Glacier have been very low at least since 1995 [27,63]. Therefore, we do not expect large variation in ice flux due to termini retreat and the latter should be driven mainly by an enhanced calving when the front retreats to deeper water in the proglacial lagoon. Thus, we associate the recent deceleration of ice thinning in the terminal part with the observed atmospheric cooling, rather than with a dynamic response to a rapid retreat to a new pinning point. However, such a possibility cannot be ruled out based on the collected data and needs further investigation.

For the long term, the frontal retreat rate is mainly controlled by the bedrock topography: water depth of the proglacial lagoon and the presence of pinning points. Additionally, the shallow depths of the proglacial lagoon (mean depth 3.6 ± 1.9 m, maximum 11.8 m) limit the ice thickness of termini and, hence, the long-term contribution of frontal retreat due to calving to observed ice loss.

The only elevation data that was able to provide glacier wide coverage of Ecology Glacier was the high resolution satellite image and DEMs from Pléiades satellite. Structure-from-Motion analysis of

archive aerial imagery did not provide reliable results in the snow-covered areas due to the low contrast and oversaturation of the photographs, while Terrestrial Laser Scanning DEM coverage suffered from shadows cast by highly undulated glacier surface.

As the bedrock topography of Ecology Glacier remains unknown, our results show only the absolute values of elevation change and cannot be expressed as percentage of the actual volume of the glacier as has been reported for other sites in South Shetland Islands (e.g., [30]). Measurements of bedrock topography would help to shed light on the future stability of the calving front and whether the observed deceleration of termini retreat will prevail or if it is just temporary and linked to the presence of an isolated pinning point [26,58] as experienced in the years 1988–2003 (Figure 10). Therefore, there is a need to extend ground penetrating radar surveys of the central part of the King George Island [36] to its peripheral icefields and outlet glaciers. This would also provide glacial geometry required for ice dynamics modelling needed for determination whether ice elevation change is driven mainly by the surface mass balance or the ice dynamics response to enhanced calving.

Acknowledgments: We would like to thank the staff of the Arctowski Polish Antarctic Station for support during field work and T. Krogulec for providing granulometry data. This study was funded within statutory activities No. 3841/E-41/S/2017 of the Ministry of Science and Higher Education of Poland. MP was partially supported by CECs, funded by the Base Finance program of CONICYT, Chile. SM and SV were supported by CONICYT-FONDECYT 11130484 and the Instituto Antártico Chileno (INACH). The open access publication has been partially financed by the Centre of Polar Studies from the funds of the Leading National Research Centre (KNOW) received for the period 2014–2018.

Author Contributions: M.P. designed the study, constructed 1979 and 2016 DEMs, and made major analysis; R.B. provided meteorological data; R.J.B. and J.S. performed and processed the oceanographic measurements; J.S. provided 2001 DEM, made DEM differentiation and maps; S.M. and S.V. provided 2012 DEM and orthophotomap; M.P. wrote the majority of the paper. All authors contributed to the final version of the manuscript.

Conflicts of Interest: The authors declare no conflict of interest. The founding sponsors had no role in the design of the study; in the collection, analyses, or interpretation of data; in the writing of the manuscript, and in the decision to publish the results.

Appendix A. TLS Locations

Table A1. TLS surveying point locations, see map on Figure 5.

Location		Date	Position (UTM 21S, EGM96)		
Name	Place		Easting (m)	Northing (m)	Elevation (m)
S1	Agat Point	17 January 2016	425,263.335	3,102,865.460	12.910
S2	Blaszczyk Moraine	10 February 2016	424,909.685	3,103,159.080	34.283
S3	Breccia Craig	14 January 2016	419,725.365	3,105,175.215	8.461
S4	Dera Icefall	14 January 2016	419,987.270	3,104,801.860	17.464
E1	Dutkiewicz Cliff E	21 March 2016	421,701.152	3,104,914.030	309.498
E2	Dutkiewicz Cliff S	21 March 2016	421,835.812	3,104,933.154	300.446
E3	Dutkiewicz Cliff W	21 March 2016	422,031.467	3,105,063.660	254.963
E4	Ecology E	17 March 2016	423,004.110	3,105,984.201	108.015
E5a	Ecology N	27 January 2016	423,413.154	3,106,413.154	51.637
E5b	Ecology N	17 March 2016	423,413.372	3,106,414.044	51.590
E6	Ecology S	17 March 2016	423,690.545	3,106,082.676	3.925
S5	Emerald Point	15 January 2016	417,086.935	3,107,134.453	10.489
S6	Kasprowy Hill	7 February 2016	421,816.623	3,105,821.195	282.570
S7	Petrified Forest	2 February 2016	423,021.155	3,107,116.456	35.822
S8	Panorama Ridge	7 February 2016	422,359.359	3,106,913.451	155.314
S9	Pond Hill	18 January 2016	416,717.283	3,105,774.282	117.998
S10	Puchalski Tomb	27 January 2016	423,430.061	3,106,697.116	56.348
S11	Rakusa Point	27 January 2016	424,041.256	3,106,611.373	4.849
E7	Wrobel Cliff	21 March 2016	422,497.392	3,105,183.933	207.595

Appendix B. Ice Elevation Change Maps

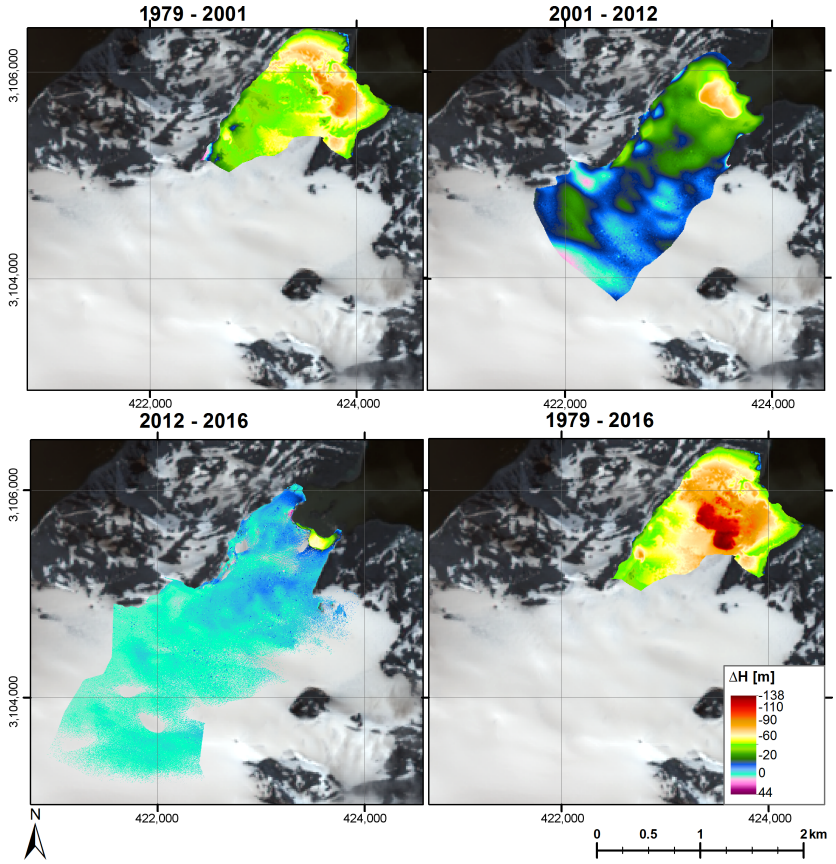

Figure A1. Changes of surface elevation of Ecology Glacier in different time periods from 1979 to 2016. Reference system: WGS 1984, UTM zone 21S, geoid EGM96.

References

1. Pfeffer, W. A simple mechanism for irreversible tidewater glacier retreat. *J. Geophys. Res. Earth Surf.* **2007**, *112*, doi:10.1029/2006JF000590.
2. Nick, F.M.; Vieli, A.; Howat, I.M.; Joughin, I. Large-scale changes in Greenland outlet glacier dynamics triggered at the terminus. *Nat.Geosci.* **2009**, *2*, 110–114.
3. Meier, M.; Post, A. Fast tidewater glaciers. *J. Geophys. Res.* **1987**, *92*, 9051–9058.
4. Vieli, A.; Funk, M.; Blatter, H. Flow dynamics of tidewater glaciers: A numerical modelling approach. *J. Glaciol.* **2001**, *47*, 595–606.
5. Howat, I.M.; Joughin, I.; Fahnestock, M.; Smith, B.E.; Scambos, T.A. Synchronous retreat and acceleration of southeast Greenland outlet glaciers 2000–06: Ice dynamics and coupling to climate. *J. Glaciol.* **2008**, *54*, 646–660.
6. Luckman, A.; Benn, D.I.; Cottier, F.; Bevan, S.; Nilsen, F.; Inall, M. Calving rates at tidewater glaciers vary strongly with ocean temperature. *Nat. Commun.* **2015**, *6*, 8566, doi:10.1038/ncomms9566 .
7. Vieli, A. Retreat instability of tidewater glaciers and marine ice sheets. In *Snow and Ice-Related Hazards, Risks and Disasters*; Haeberli, W., Whiteman, C., Eds.; Elsevier: Amsterdam, The Netherlands, 2014; pp. 677–712.
8. Minowa, M.; Sugiyama, S.; Sakakibara, D.; Skvarca, P. Seasonal Variations in Ice-Front Position Controlled by Frontal Ablation at Glaciar Perito Moreno, the Southern Patagonia Icefield. *Front. Earth Sci.* **2017**, *5*, 1.
9. Motyka, R.J.; Cassotto, R.; Truffer, M.; Kjeldsen, K.K.; van As, D.; Korsgaard, N.J.; Fahnestock, M.; Howat, I.; Langen, P.L.; Mortensen, J.; et al. Asynchronous behavior of outlet glaciers feeding Godthåbsfjord (Nuup Kangerlua) and the triggering of Narsap Sermia's retreat in SW Greenland. *J. Glaciol.* **2017**, *63*, 288–308.
10. Oerlemans, J.; Nick, F. A minimal model of tidewater glacier. *Ann. Glaciol.* **2005**, *42*, 1–6.

11. Roe, G.H.; Baker, M.B.; Herla, F. Centennial glacier retreat as categorical evidence of regional climate change. *Nat. Geosci.* **2016**, *10*, 95–99.
12. Scambos, T.; Berthier, E.; Haran, T.; Shuman, C.; Cook, A.; Ligtenberg, S.; Bohlander, J. Detailed ice loss pattern in the northern Antarctic Peninsula: widespread decline driven by ice front retreats. *Cryosphere* **2014**, *8*, 2135–2145.
13. Zemp, M.; Frey, H.; Gärtner-Roer, I.; Nussbaumer, S.U.; Hoelzle, M.; Paul, F.; Haeberli, W.; Denzinger, F.; Ahlstrøm, A.P.; Anderson, B.; et al. Historically unprecedented global glacier decline in the early 21st century. *J. Glaciol.* **2015**, *61*, 745–762.
14. Oerlemans, J. Extracting a climate signal from 169 glacier records. *Science* **2005**, *308*, 675–677.
15. Vaughan, D.; Marshall, G.; Connolley, W.; Parkinson, C.; Mulvaney, R.; Hodgson, D.; King, J.; Pudsay, C.; Turner, J. Recent rapid regional climate warming on the Antarctic Peninsula. *Clim. Chang.* **2003**, *60*, 243–274.
16. Rignot, E.; Casassa, G.; Gogineni, P.; Krabill, W.; Rivera, A.U.; Thomas, R. Accelerated ice discharge from the Antarctic Peninsula following the collapse of Larsen B ice shelf. *Geophys. Res. Lett.* **2004**, *31*, doi:10.1029/2004GL020697.
17. Pritchard, H.; Vaughan, D. Widespread acceleration of tidewater glaciers on the Antarctic Peninsula. *J. Geophys. Res.* **2007**, *112*, F03S29.
18. Turner, J.; Lu, H.; White, I.; King, J.; Phillips, T.; Hosking, J.; Bracegirdle, T.; Marshall, G.; Mulvaney, R.; Deb, P. Absence of 21st century warming on Antarctic Peninsula consistent with natural variability. *Nature* **2016**, *535*, 411–415.
19. Oliva, M.; Navarro, F.; Hrbáček, F.; Hernández, A.; Nývlt, D.; Pereira, P.; Ruiz-Fernández, J.; Trigo, R. Recent regional climate cooling on the Antarctic Penisula and associated impacts on the cryosphere. *Sci. Total Environ.* **2017**, *580*, 210–223.
20. Navarro, F.; Jonsell, U.; Corcuera, M.; Martin-Espanol, A. Decelerated mass loss of Hurd and Johnsons Glaciers, Livingston Island, Antarctic Peninsula. *J. Glaciol.* **2013**, *59*, 115–128.
21. Arctic and Antarctic Research Institute, St. Petersburg. 2017. Available online: http://www.aari.aq/data/data.php?lang=1&station=0 (accessed on 18 April 2017).
22. Hock, R.; de Woul, M.; Radić, V.; Dyurgerov, M. Mountain glaciers and ice caps around Antarctica make a large sea-level rise contribution. *Geophys. Res. Lett.* **2009**, *36*, L07501.
23. Van den Broeke, M.; Enderlin, E.; Howat, I.; Kuipers Munneke, P.; Noël, B.; van de Berg, W.; van Meijgaard, E.; Wouters, B. On the recent contribution of the Greenland ice sheet to sea level change. *Cryosphere* **2016**, *10*, 1933–1946.
24. Marinsek, S.; Ermolin, E. 10 year mass balance by glaciological and geodetic methods of Glaciar Bahía del Diablo, Vega Island, Antarctic Peninsula. *Ann. Glaciol.* **2015**, *56*, 141–146.
25. Simões, J.; Bremer, U.; Aquino, F.; Ferron, F. Morphology and variations of glacial drainage basins in the King George Island ice field, Antarctica. *Ann. Glaciol.* **1999**, *29*, 220–224.
26. Rückamp, M.; Braun, M.; Suckro, S.; Blindow, N. Observed glacial changes on the King George Island ice cap, Antarctica, in the last decade. *Glob. Planet. Chang.* **2011**, *79*, 99–109.
27. Osmanoglu, B.; Braun, M.; Hock, R.; Navarro, F. Surface velocity and ice discharge of the ice cap on King George Island, Antarctica. *Ann. Glaciol.* **2013**, *54*, 111–119.
28. Sobota, I.; Kejna, M.; Araźny, A. Short-term mass changes and retreat of the Ecology and Sphinx glacier system, King George Island, Antarctic Peninsula. *Antarct. Sci.* **2015**, *27*, 500–510.
29. Cielos, R.R.; de Mata, J.A.; Galilea, A.D.; Alonso, M.Á.; Cielos, P.R.; Valero, F.N. Geomatic methods applied to the study of the front position changes of Johnsons and Hurd Glaciers, Livingston Island, Antarctica, between 1957 and 2013. *Earth Syst. Sci. Data* **2016**, *8*, 341–353.
30. Molina, C.; Navarro, F.; Calvet, J.; García-Sellés, D.; Lapazaran, J. Hurd Peninsula glaciers, Livingston Island, Antarctica, as indicators of regional warming: ice-volume changes during the period 1956–2000. *Ann. Glaciol.* **2007**, *46*, 43–49.
31. Bliss, A.; Hock, R.; Cogley, J. A new inventory of mountain glaciers and ice caps for the Antarctic periphery. *Ann. Glaciol.* **2013**, *54*, 191–199.
32. Braun, M.; Hock, R. Spatially distributed surface energy balance and ablation modelling on the ice cap of King George Island (Antarctica). *Glob. Planet. Chang.* **2004**, *42*, 45–58.
33. Knap, W.; Oerlemans, J.; Cadée, M. Climate sensitivity of the ice cap of King George Island, South Shetland Islands, Antarctica. *Ann. Glaciol.* **1996**, *23*, 154–159.

34. Pfeffer, W.T.; Arendt, A.A.; Bliss, A.; Bolch, T.; Cogley, J.G.; Gardner, A.S.; Hagen, J.O.; Hock, R.; Kaser, G.; Kienholz, C.; et al. The Randolph Glacier Inventory: A globally complete inventory of glaciers. *J. Glaciol.* **2014**, *60*, 537–552.
35. Macheret, Y.; Moskalevsky, M. Study of Lange Glacier on King George Island, Antarctica. *Ann. Glaciol.* **1999**, *29*, 202–206.
36. Blindow, N.; Suckro, S.; Ruckamp, M.; Braun, M.; Breuer, B.; Saurer, H.; Simoes, J.; Schindler, M.; Lange, M. Geometry and thermal regime of the King George Island ice cap, Antarctica, from GPR and GPS. *Ann. Glaciol.* **2010**, *51*, 103–109.
37. Bintanja, R. The local surface energy balance of the Ecology Glacier, King George Island, Antarctica: Measurements and modelling. *Antarct. Sci.* **1995**, *7*, 315–325.
38. Mieczan, T.; Górniak, D.; Świątecki, A.; Zdanowski, M.; Tarkowska-Kukuryk, M.; Adamczuk, M. Vertical microzonation of ciliates in cryoconite holes in Ecology Glacier, King George Island. *Pol. Polar Res.* **2013**, *34*, 201–212.
39. Zdanowski, M.; Żmuda-Baranowska, M.; Borsuk, P.; Świątecki, A.; Górniak, D.; Wolicka, D.; Jankowska, K.; Grzesiak, J. Culturable bacteria community development in postglacial soils of Ecology Glacier, King George Island, Antarctica. *Polar Biol.* **2013**, *36*, 511–527.
40. Muser, D. Der Gletscherrückzug auf King George Island, South Shetland Islands Zwischen 1956 und 1992. Eine Digitale Auswertung von Karten, Luftbildern und Satellitendaten. Ph.D. Thesis, Albert-Ludwigs-Universität Freiburg, Freiburg im Breisgau, Germany, 1995.
41. Birkenmajer, K. Retreat of Ecology Glacier, Admiralty Bay, King George Island (South Shetland Islands, West Antarctica), 1956–2001. *Bull. Pol. Acad. Sci. Earth Sci.* **2002**, *50*, 15–29.
42. Rosa, K.; Vieira, R.; Simões, J. Dinâmica glacial e características sedimentares resultantes na zona proglacial da geleira Ecology-Baía do Almirantado, ilha Rei George-Antártica. *Rev. Bras. Geomorfol.* **2006**, *7*, 51–60.
43. Battke, Z. *Admiralty Bay, 1:50000 Scale (Explanations in Polish)*; Printed WZKart: Warsaw, Poland, 1980.
44. Pudełko, R. Two new topographic maps for sites of scientific interest on King George Island, West Antarctica. *Pol. Polar Res.* **2008**, *29*, 291–297.
45. Pudełko, R. Topographic map of the SSSI No. 8, King George Island, West Antarctica. *Pol. Polar Res.* **2003**, *24*, 53–60.
46. Westoby, M.; Brasington, J.; Glasser, N.; Hambrey, M.; Reynolds, J. 'Structure-from-Motion' photogrammetry: A low-cost, effective tool for geoscience applications. *Geomorphology* **2012**, *179*, 300–314.
47. Midgley, N.; Tonkin, T. Reconstruction of former glacier surface topography from archive oblique aerial images. *Geomorphology* **2017**, *282*, 18–26.
48. Battke, Z. *Admiralty Bay. King George Island, 1:50000 Scale*; E Romer State Cartographic Publishing House: Warsaw, Poland, 1990.
49. Berthier, E.; Vincent, C.; Magnússon, E.; Gunnlaugsson, A.; Pitte, P.; Le Meur, E.; Masiokas, M.; Ruiz, L.; Palsson, F.; Belart, J.; et al. Glacier topography and elevation changes derived from Pléiades sub-meter stereo images. *Cryosphere* **2014**, *8*, 2275–2291.
50. Marti, R.; Gascoin, S.; Berthier, E.; de Pinel, M.; Houet, T.; Laffly, D. Mapping snow depth in open alpine terrain from stereo satellite imagery. *Cryosphere* **2016**, *10*, 1361–1380.
51. Gabbud, C.; Micheletti, N.; Lane, S. Lidar measurement of surface melt for a temperate Alpine glacier at the seasonal and hourly scales. *J. Glaciol.* **2015**, *61*, 963–974.
52. Fischer, M.; Huss, M.; Kummert, M.; Hoelzle, M. Application and validation of long-range terrestrial laser scanning to monitor the mass balance of very small glaciers in the Swiss Alps. *Cryosphere* **2016**, *10*, 1279–1295.
53. Koppes, M.; Hallet, B.; Rignot, E.; Mouginot, J.; Wellner, J.S.; Boldt, K. Observed latitudinal variations in erosion as a function of glacier dynamics. *Nature* **2015**, *526*, 100–103.
54. Navarro, F.; Glazovsky, A.; Macheret, Y.; Vasilenko, E.; Corcuera, M.; Cuadrado, M. Ice-volume changes (1936–1990) and structure of Aldegondabreen, Spitsbergen. *Ann. Glaciol.* **2005**, *42*, 158–162.
55. Paul, F.; Haeberli, W. Spatial variability of glacier elevation changes in the Swiss Alps obtained from two digital elevation models. *Geophys. Res. Lett.* **2008**, *35*.
56. Nuth, C.; Kääb, A. Co-registration and bias corrections of satellite elevation data sets for quantifying glacier thickness change. *Cryosphere* **2011**, *5*, 271.
57. Falk., U.; Sala, H. Winter melt conditions of the inland ice cap on King George Island, Antarctic Peninsula. *Erdkunde* **2015**, *69*, 341–363.

58. Vieli, A.; Jania, J.; Kolondra, L. The retreat of a tidewater glacier: Observations and model calculations on Hansbreen, Spitsbergen. *J. Glaciol.* **2002**, *48*, 592–600.
59. Kirkbride, M.; Warren, C. Calving processes at a grounded ice cliff. *Ann. Glaciol.* **1997**, *24*, 116–121.
60. O'Leary, M.; Christoffersen, P. Calving on tidewater glacier amplified by submarine frontal melting. *Cryosphere* **2013**, *7*, 119–128.
61. Pętlicki, M.; Ciepły, M.; Jania, J.; Promińska, A.; Kinnard, C. Calving of a tidewater glacier driven by melting at the waterline. *J. Glaciol.* **2015**, *61*, 851–863.
62. Braun, M.; Saurer, H.; Vogt, S.; Simoes, J.; Gossman, H. The influence of large-scale atmospheric circulation on the surface energy balance of the King George Island ice cap. *Int. J. Climatol.* **2001**, *21*, 21–36.
63. Moll, A.; Braun, M. Determination of Glacier Velocities on King George Island (Antarctica) by DinSAR. In Proceedings of the International Geoscience and Remote Sensing Symposium (IGARSS 2006), Denver, CO, USA, 31 July–4 August 2006.